HOT PLASMA RAY TRACING OF ELECTROMAGNETIC AND ELECTROSTATIC WAVES IN THE MAGNETOSPHERE

Akira SAWADA, Iwane KIMURA and Yoshiya KASAHARA

Department of Electrical Engineering II, Kyoto University
Kyoto 606, JAPAN

1 Introduction

To investigate various wave phenomena in the magnetosphere, ray tracing method has been used as a powerful tool. Especially, ray paths of whistler mode waves are calculated by many researchers and the results have contributed to many physical interpretations of natural and artificial wave phenomena. However, in most cases the magnetospheric plasma is treated as a cold plasma and the thermal effect of a particle motion is neglected in the ray tracing. This treatment becomes inappropriate when we calculate ray paths of the waves which are strongly affected by the thermal motion, such as electrostatic waves. In recent years, we have been developed a complete computer program for three dimensional (3-D) ray tracing in a hot plasma, which can deal with electrostatic waves as well as electromagnetic waves in the magnetospheric plasma [*Hashimoto et al.*, 1987].

In the present paper, we describe our further extended ray tracing program in which multi-component plasmas such as a loss-cone plasma and a thermal effect of ions are taken into account applicable to the ray tracing of ion-mode waves. We will also show several examples of the hot plasma ray tracing.

2 Techniques for hot plasma ray tracing

The fundamental equations for ray tracing are

$$\frac{d\boldsymbol{r}}{d\tau} = \frac{\partial D}{\partial \boldsymbol{k}} , \tag{1}$$

$$\frac{d\boldsymbol{k}}{d\tau} = -\frac{\partial D}{\partial \boldsymbol{r}} , \tag{2}$$

$$\frac{dt}{d\tau} = -\frac{\partial D}{\partial \omega} , \tag{3}$$

where $\boldsymbol{r}$, $\boldsymbol{k}$, t, ω and τ are the position vector on the ray path, the wave number vector, the propagation time, the angular frequency of the wave and a parameter proportional to the path element, respectively.

The dispersion function $D(\omega, \boldsymbol{k}, \boldsymbol{r})$ in equations (1) – (3) must be constant along the ray path, where we assume that D is independent of time t. We can introduce the thermal effect of a particle motion in a hot plasma into the dispersion function D. To calculate D numerically we adopt a bi-Maxwellian velocity distribution function for each plasma component. For example, we assume that the plasma medium consists of two component; one is a thermal plasma component in the background with a temperature of 500K and the other is a loss-cone hot plasma component as an energy source of electrostatic waves. The velocity distribution of the loss-cone component is a subtracted bi-Maxwellian distribution which is represented as a difference of two bi-Maxwellian distributions [*Ashour-abdalla and Kennel*, 1978]. The dispersion relation in this plasma is shown in Fig. 1 as a so-called $\omega - k$ diagram. The wave frequency ω and the wave number k are normalized by the electron cyclotron frequency Ω_e and the Larmor radius of the hot plasma component ρ_H. The electron plasma frequency Π_e is $3.52\Omega_e$, in which the loss-cone plasma has a half contribution. Temperature of the hot plasma component is 10,000K. To solve the dispersion relation $D(\omega, k) = 0$ numerically, we adopt the Muller method. As for the detail derivation of the dispersion function of a bi-Maxwellian plasma, you can refer to *Hashimoto et al.* [1987].

When the propagation medium is unstable, the dispersion relation has complex solutions in general. In our ray tracing, we assume the wave frequency ω to be real, so that the wave number $\boldsymbol{k}$ becomes a complex value $\boldsymbol{k}_r + \mathrm{i}\,\boldsymbol{k}_i$. The imaginary part $\boldsymbol{k}_i$ is considered as a spatial growth rate of the wave

amplitude, so that we calculate a total growth or damping along a ray path as follows:

$$\Gamma = -\int_{\text{path}} \boldsymbol{k}_{\text{i}} \cdot \mathrm{d}\boldsymbol{r} = -\int_{\text{path}} \boldsymbol{k}_{\text{i}} \cdot \boldsymbol{v}_{\text{g}} \mathrm{d}t \ , \tag{4}$$

where $\boldsymbol{v}_{\text{g}}$ is the group velocity.

3 Ray paths of electron cyclotron harmonic waves

As an example of the hot plasma ray tracing, we calculate ray paths of electron cyclotron harmonic waves (ECHW) under the hot plasma condition corresponding to the $\omega - k$ diagram shown in Fig. 1. It should be noted that the ECHW branches have two resonance points f_{q1} and f_{q2} on each branch, and an unstable region due to the electron cyclotron instability exists around the second resonance point f_{q2}. The resonance point f_{q1} is due to the loss-cone distribution of 10,000K and f_{q2} is due to the thermal plasma of 500K. In this case, third harmonics of the ECHW connects to the UHR wave through f_{q1} resonance and finally reaches the point W called a radio window, where the L–X mode waves couple with the L–O mode waves. A mode conversion theory along this dispersion curve was proposed as a generation mechanism of Terrestrial Miriametric Radiation (TMR) by *Jones* [1976]. *Hashimoto et al.* [1987] confirm this theory by calculating ray paths of such waves using hot plasma ray tracing.

In the present study, we calculate ray paths starting from the radio window where the wave frequency is equal to the local electron plasma frequency and the ray propagates to a larger k region. Fig. 2(a) shows a ray path starting from the geocentric distance $r = 3.20\, r_{\text{e}}$ (r_{e}: the earth radius) on the geomagnetic equatorial plane. Attached arrows correspond to the directions of the wave normal which is parallel to the geomagnetic field line in the initial state. The ray propagates northwards with increasing its wave normal angle to the magnetic field line and the wave frequency becomes close to the local UHR frequency. After the ray reflects back sharply at the point f_{q1}, the wave propagates as a backward wave and then gradually the wave changes its propagating direction. At the point f_{q2}, the direction of propagation becomes backward again. In this final stage the wave grows its amplitude over 40dB.

To compare with this result, Fig. 2(b) shows a ray path calculated in a single bi-Maxwellian plasma of 1eV. In this case, the second resonance point f_{q2} disappears, so that the ray propagates backward after it passes the f_{q1} resonance point, and does not become forward propagating wave. At the end of calculation of this ray path, ray tracing is terminated by the condition of $|k_{\text{i}}/k_{\text{r}}| > 10^{-2}$. This means that the wave is strongly damped by the cyclotron damping and at the same time the ray tracing becomes meaningless. In the calculation of the ray path shown in Fig. 2(a), the ratio $|k_{\text{i}}/k_{\text{r}}|$ stays below 10^{-3} at all times. These characteristics of ray paths strongly depend on the starting locations. When the initial points are almost 1° in latitude off from the geomagnetic equatorial plane, the waves are severely damped before reaching the f_{q2} resonance point.

4 Ray paths of ion-mode waves

Ion-mode waves in the electromagnetic region can be classified into several modes and their ray paths show considerably different characteristics in each mode. *Rauch and Roux* [1982] took account of two species of ions, i.e., H^+ and He^+ and calculated ray paths of three types of ULF waves in a geomagnetic meridian plane. Fig. 3 shows an $\omega - k$ diagram of these ion-mode waves. The quantities $\Omega_{\text{H+}}$ and V_{A} are the gyro frequency of H^+ and the Alfvén velocity, respectively. In our 3-D hot plasma ray tracing program, thermal effects of ion motion can be also taken into account. Ray paths shown in Fig. 4(a) and (b) are the results of our hot plasma ray tracing of class 1 and class 3 waves (see Fig. 3), respectively. In this calculation, we consider four species of particles, that is, thermal electrons (1.5eV), thermal H^+ (1.5eV), thermal He^+ (1.5eV) and hot H^+ (15keV). In both cases, the starting points are $r = 6.5\, r_{\text{e}}$ on the geomagnetic equatorial plane and the initial wave normal directions are assumed to be parallel to the magnetic field line.

The ray of class 1 wave propagates along the same field line indicated by a thin broken line and reaches the ionosphere. The density profile model used in the present calculation does not take account of the effect of F region in the ionosphere, so that ray tracing is terminated at that point. On the other hand, the ray of class 3 wave is trapped in the region where r is higher than $6r_{\text{e}}$. The reflection at the north edge of the path is caused by the lower hybrid resonance due to He^+ ions. These results are almost same with *Rauch and Roux*'s [1982]. Moreover using the hot plasma ray tracing, we can estimate the wave amplification along the paths. Both waves in class 1 and class 3 have a growth rate due to the ion cyclotron instability when the wave normal direction is close to the magnetic field line. However,

magnitude of the growth rate is bigger for class 1 waves than for class 3 waves in the present plasma parameters, so that, waves in class 1 is amplified almost 5dB, while class 3 waves have little gain along the path. As compared with the growth of the ECHW mentioned in the previous section, total growth of the amplitude is considerably small, because the wave normal directions deviate soon from the direction of the geomagnetic field line within a short propagation distance.

For ion-mode ray tracing, it must be carefully checked whether or not the WKB approximation is valid throughout the path. Actually, however, it is confirmed that the wave length is sufficiently shorter than a scale of the medium change.

5 Summary

Using the hot plasma ray tracing program developed in the present study, we can calculate a ray path of any electromagnetic and electrostatic waves with the evaluation of a total growth/damping along the path in an arbitrary plasma distribution which is expressed as a sum or difference of bi-Maxwellian distribution. This powerful tool will provide us with a lot of information, when we interpret wave data observed by satellites and on the ground.

Acknowledgements

The authors wish to express their sincere thanks to Drs. H. Matsumoto and Y. Omura at RASC, Kyoto Univ. for their valuable discussions and comments.

References

Ashour-Abdalla, M. and C. F. Kennel, Nonconvective and Convective electron cyclotron harmonic instabilities, *J. Geophys. Res.*, *83*, 1531, 1978.

Hashimoto, K., K. Yamaashi, and I. Kimura, Three-dimensional ray tracing of electrostatic cyclotron harmonic waves and Z mode electromagnetic waves in the magnetosphere, *Radio Sci.*, *22*, 579, 1987.

Jones, D., Source of terrestrial non-thermal radiation, *Nature*, *260*, 686, 1976.

Rauch, J. L., and A. Roux, Ray tracing of ULF waves in a multicomponent magnetospheric plasma: consequences for the generation mechanism of ion cyclotron waves, *J. Geophys. Res.*, *87*, 8191, 1982.

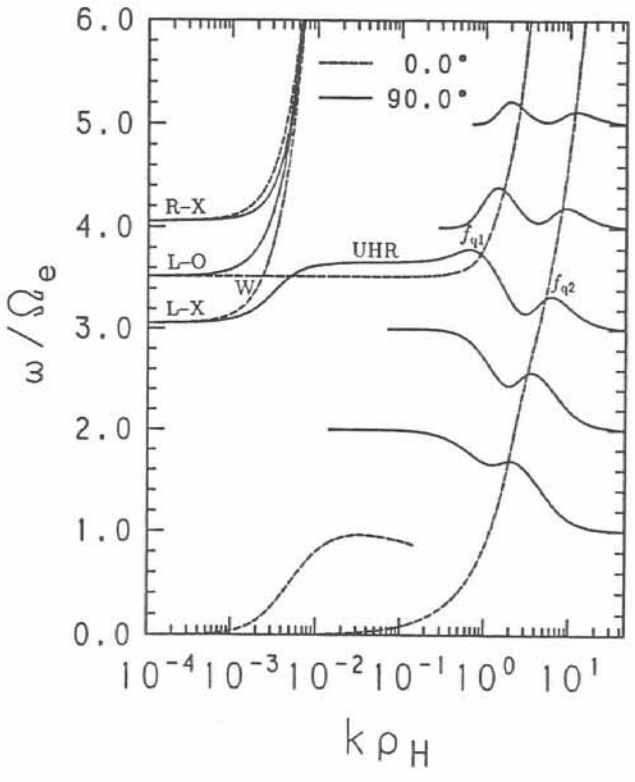

Fig. 1. A $\omega - k$ diagram of electron-mode waves in a multi-component loss-cone plasma.

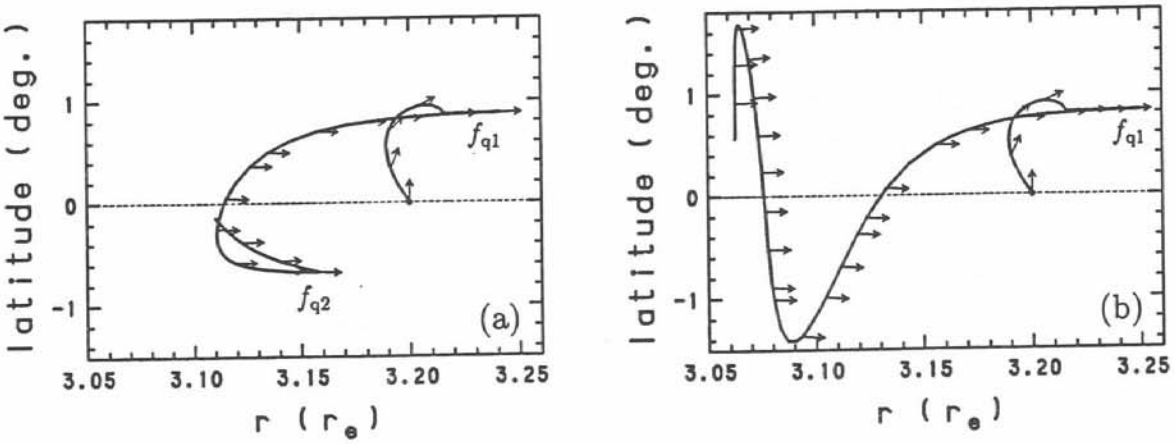

Fig. 2. Ray paths of electrostatic electron cyclotron harmonic waves near the geomagnetic equator in (a) a multi-component loss-cone plasma and (b) a single bi-Maxwellian plasma.

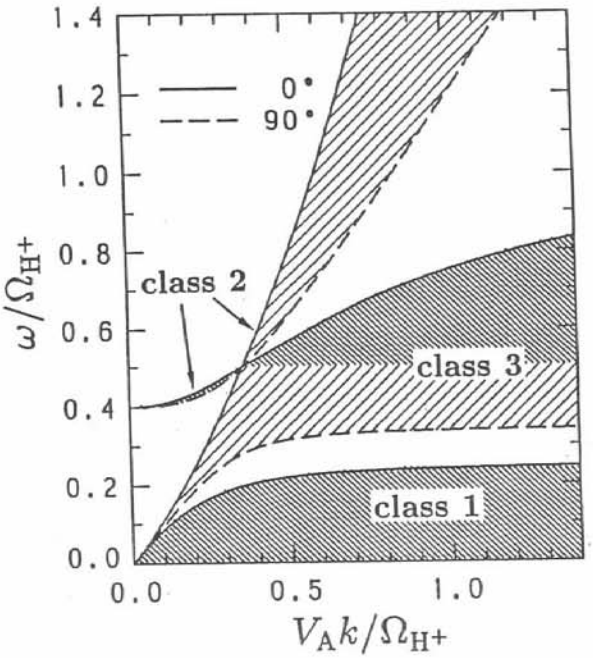

Fig. 3. A $\omega-k$ diagram of ion-mode waves in a plasma consisting of H^+, He^+ and electrons.

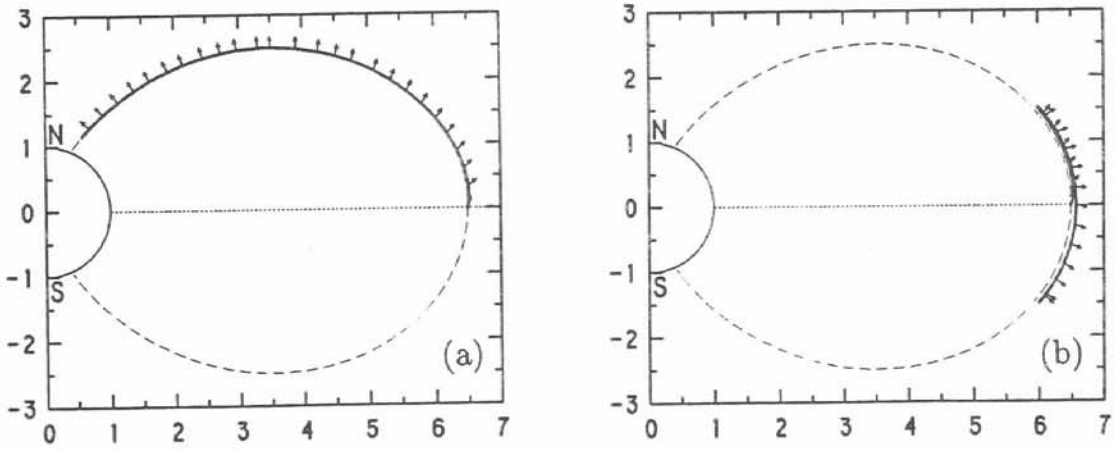

Fig. 4. Ray path of ion-mode waves in (a) class 1 and (b) class 3 of Fig. 3.